JOURNAL OF SOLID STATE CHEMISTRY 70, 235–240 (1987)

Structure and Properties of Triclinic $Ni_{0.85}Mo_6Te_8$*

W. HÖNLE† AND K. YVON

Laboratoire de Cristallographie aux Rayons X, Université de Genève, 24, quai Ernest-Ansermet, CH-1211 Geneva 4, Switzerland

Received November 3, 1986

The structure of $Ni_{0.85}Mo_6Te_8$ was refined from single-crystal X-ray diffraction data at room temperature. It is triclinic, space group $P\bar{1}$, a = 7.028(2) Å, b = 7.100(2) Å, c = 7.102(2) Å, α = 91.23(2)°, β = 95.73(2)°, γ = 90.82(2)°, V = 352.48 Å^3, Z = 1; 1619 reflections, 75 refined parameters, R = 0.031. The Mo atoms form distorted octahedral clusters (2.69 Å $\leq d_{intra}$[Mo–Mo] $\leq$ 2.81 Å; 3.58 Å < d_{inter}[Mo–Mo]). The Ni atoms are disordered (site occupancy: 0.423(7); d[Ni–Ni] = 2.586(6) Å), and interact strongly with one Mo_6 cluster (d[Ni–Mo] = 2.603(3) and 2.958(3) Å), and weakly with another (d[Ni–Mo] = 2.985(3) Å). The structure transforms at 1057(5) K into a rhombohedral modification (a_{hex} = 10.457(2) Å, c_{hex} = 11.866(3) Å at 1073 K). Measurements on powders suggest metallic conductivity (5.1×10^{-4} Ω-cm at 293 K) and weakly temperature-dependent paramagnetism (110×10^{-6} emu/g at 100 K).

1. Introduction

Chevrel phases $M_xMo_6X_8$ (M_x = metal, X = chalcogen) based on tellurium are relatively rare. Tellurides have so far only been reported for M_x = Fe ($0 < x < 2$), Co ($0 < x < 0.66$), Ni ($0 < x < 2$), and Cu ($0 < x < 2$) (*1*). Their crystal symmetries at room temperature were either rhombohedral (Fe, Co) or triclinic (Ni, Cu). Apart from lattice parameters for the Fe- and Co-containing compounds no other information was given.

In this communication we report on a structural characterization and some properties of triclinic $Ni_{0.85}Mo_6Te_8$. Preliminary results were presented elsewhere (*2*).

* Dedicated to Dr. H. Nowotny.

† On leave from Max-Planck Institut für Festkörperforschung, Stuttgart, Federal Republic of Germany.

2. Experimental and Results

A sample of nominal composition $NiMo_6Te_8$ was prepared by reaction of binary Mo_6Te_8 with elemental Ni at 1300 K in sealed quartz ampoules. The preparation of Mo_6Te_8 was described previously (*3*). X-ray Guinier photographs confirmed the formation of a new ternary compound. The intensity profile was similar to that of rhombohedral Mo_6Te_8 (a_r = 7.10 Å, α_r = 92.60°; according to Ref. (*1*); a_r = 7.050(3) Å, α_r = 92.54(3)°, V_r = 349.3 Å^3, according to Ref. (*4*)), except for line splitting which suggested a triclinic lattice distortion. A single crystal of approximately cubic shape (edge lengths ≈ 0.02 mm) was isolated and examined on an automated four-circle X-ray diffractometer. Cell parameters (see abstract) were determined by least-squares refinement of 12 measured Bragg angles in the region $15° \leq 2\theta < 25°$. Integrated inten-

0022-4596/87 $3.00

TABLE I

ATOMIC PARAMETERS

Atom	x	y	z	$U_{eq.}$	U_{11}	U_{33}	U_{22}	U_{23}	U_{12}	U_{13}
Mo(1)	0.2423(1)	0.4239(1)	0.5411(1)	76(2)	60(4)	72(4)	95(4)	−5(3)	7(3)	6(3)
Mo(2)	0.4108(1)	0.5499(1)	0.2434(1)	83(2)	65(4)	88(4)	95(4)	−1(3)	1(3)	3(3)
Mo(3)	0.5432(1)	0.2376(1)	0.4228(1)	88(2)	75(4)	99(4)	91(4)	4(3)	5(3)	24(3)
Te(1)	0.1034(1)	0.7463(1)	0.3621(1)	120(2)	86(3)	107(3)	173(4)	24(2)	40(2)	26(2)
Te(2)	0.7344(1)	0.3721(1)	0.1314(1)	105(2)	95(3)	124(3)	95(3)	−8(2)	7(2)	20(2)
Te(3)	0.3973(1)	0.1157(1)	0.7509(1)	142(2)	173(4)	88(3)	176(3)	−26(2)	77(3)	−27(2)
Te(4)	0.2020(1)	0.2237(1)	0.1968(1)	126(2)	94(3)	113(3)	168(3)	−1(2)	−12(2)	−9(2)
Ni	0.1718(4)	0.0645(4)	0.4916(4)	116(9)	87(16)	118(16)	143(16)	−1(11)	6(11)	−1(11)

Note. $Ni_{0.85}Mo_6Te_8$, $a = 7.028(2)$ Å, $b = 7.100(2)$ Å, $c = 7.102(2)$ Å, $\alpha = 91.23(2)°$, $\beta = 95.73(2)°$, $\gamma = 90.82(2)°$, $P\bar{1}$ (No. 2), $Z = 1$, 1619 *hkl*, d(calc) = 7.753 g/cm^3, $R = 0.031$, all atoms in 2(*a*), PP(Ni) = 0.423(7). The U_{ij} (Å^2 × 100) are expressed as $\exp -2\pi^2(h^2a^{*2}U_{11} + \cdots + 2hka^*b^*U_{12})$. $U_{eq.}$ is defined as one-third of the trace of the orthogonalized U_{ij} tensor.

sities of 1619 symmetry-independent reflections were collected at room temperature in the range $3° \leq 2\theta \leq 55°$ by using continuous $\theta - 2\theta$ scans and graphite monochromatized Mo$K\alpha$ radiation. Absorption effects (μ[Mo$K\alpha$] = 244 cm^{-1}) were corrected empirically from azimuthal scans of 11 reflections. The structure was solved by direct methods in space group $P\bar{1}$ (380 $E(hkl)$ values with $E \geq 1.20$; 2494 triple-product relations; tests for negative-quartet relations) and refined by conventional least-squares methods. The weighting scheme used was $w = 1/([\sigma(F)]^2 + 0.0002F^2)$. The position of the Ni atoms was derived from Fourier maps. Preliminary refinements with isotropic temperature factors and fixed occupancy of the Ni atom site (PP(Ni) = 0.5) converged at $R = 0.072$. Subsequent refinements with anisotropic temperature factors and variable occupancy of the Ni atom site converged at $R = 0.031$. The refined occupancy factor, PP(Ni) = 0.423(7), indicated that the crystal was Ni deficient compared to the overall sample composition and that its stoichiometry was $Ni_{0.85(2)}Mo_6Te_8$. Refinements based on an ordered Ni atom distribution (PP(Ni) = 1.0) in noncentrosymmetric space group $P1$ gave a poorer fit ($R = 0.037$). All calculations were performed using the program system SHELXTL (*5*). Atomic parameters are summarized in Table I, and a structural drawing is given in Fig. 1.[1] For comparison with rhombohedral Mo_6Te_8 (space group $R\bar{3}$) the structure was described such that its pseudotrigonal axis runs along [111]. This nonstandardized (*6*) description corresponds to that adopted in work on other triclinic Chevrel phases (see below).

The stability of $Ni_{0.85}Mo_6Te_8$ at high tempearture was studied by differential thermal analysis (DTA) performed on a NETZSCH DTA 404S apparatus. Approximately 150 mg of finely ground powder was placed in a quartz ampoule which was evacuated and sealed under vacuum. The heating rate was 10 K/min and the maximum heating temperature 1473 K. Upon heating two endothermic peaks were observed, one occurring at 1057(5) K and the other at 1216(5) K. The intensity of the

[1] Additional material to this paper can be ordered from Pachinformationszentrum Energie Physik Mathematik, D-7514 Bggenstein-Leopoldshafen-2, Federal Republic of Germany, by referring to the authors and title of the paper.

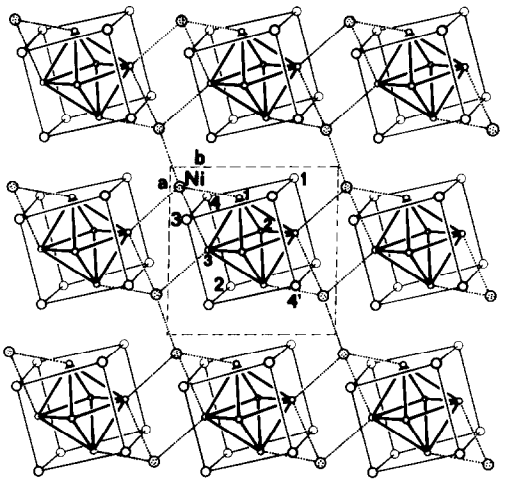

FIG. 1. Projection on a–b plane of $Ni_{0.85}Mo_6Te_8$. Small open circles, Mo; large open circles, Te; dotted circles, Ni atom sites (occupancy: 42%). Atom numbering as in Table I. The pseudo-trigonal axis runs through Te4 and Te4'. Thick lines, Mo–Mo bonds; dotted lines, Mo–Ni and Ni–Ni bonds; thin lines, Te–Te contacts indicating the $[Mo_6Te_8]$ units.

latter peak was approximately one-fifth that of the former. High-temperature X-ray powder photographs (Simon-Guinier camera) taken at 1073 and 1243 K suggested that the first DTA peak was due to a structural phase transition leading to a modification of rhombohedral symmetry. Its hexagonal lattice parameters (see abstract) were determined at 1073 K from 19 *hkl* values in the region $25° \leq 2\theta < 72°$.

The diffraction profile showed good agreement with a theoretical powder pattern calculated for rhombohedral Mo_6Te_8 (*4*) containing one Ni atom at the inversion center of the chalcogen atom network. The nature of the second DTA peak was not clarified. Upon cooling, both DTA peaks showed a hysteresis of about 13 K, confirming the first-order nature of the structural phase transition. X-ray photographs taken after the DTA experiment showed that the transition was reversible.

The electrical resistivity was measured on a sintered pellet by the four-point method in the temperature range between 298 and 2.5 K. It decreased continuously from 5.1×10^{-4} Ω-cm at room temperature to 2.8×10^{-4} Ω-cm at 2.5 K, suggesting metallic conductivity.

The magnetic susceptibility was measured on a polycrystalline powder sample as a function of temperature (T = 6–300 K, applied field 1000*G*), and magnetic field (5–50 kG, T = 5–300 K) by using a SQUID magnetometer (*7*). It decreased from 140×10^{-6} emu/g (300 K) to 110×10^{-6} emu/g (100 K) and then increased to 250×10^{-6} emu/g (4 K). A diamagnetic correction of -210×10^{-6} emu/g was applied. No variation as a function of applied field was observed. The susceptibility increase below T = 50 K was attributed to the presence of about 0.3% of metallic Ni, a value which is consistent with the observed Ni deficiency (0.5 mole%) of the triclinic structure.

3. Discussion

Triclinic $Ni_{0.85}Mo_6Te_8$ is isostructural to its selenium-based congener $Ni_{0.66}Mo_6Se_8$ (*8*). The structures differ mainly with respect to their triclinic lattice shears relative to their rhombohedral (high-temperature) modification: $a < b$, $b \simeq c$; $\alpha \simeq \gamma < \beta$ ($Ni_{0.85}Mo_6Te_8$); $b < a$, $a \simeq c$; $\alpha \simeq \gamma < \beta$ ($Ni_{0.66}Mo_6Se_8$), thus leading to different standardized (*6*) structure descriptions (L. Gelato, personal communication). The structure is built up by cube-shaped $[Mo_6Te_8]$ units (Fig. 1) which contain triclinic distorted octahedral Mo_6 clusters (2.688(1) Å $< d_{intra}$[Mo–Mo] $\leq$ 2.812(1) Å (telluride); 2.650 Å $< d_{intra}$[Mo–Mo] $<$ 2.818 Å (selenide)). The average Mo–Mo bond length within the Mo_6 clusters in the telluride (d_{av}[Mo–Mo] = 2.74 Å) is almost identical to that in the corresponding Ni-free binary compound Mo_6Te_8 (d_{av}[Mo–Mo] = 2.74 Å (*4*)), whereas that in the selenide (d_{av}[Mo–Mo] = 2.73 Å) it is

TABLE II

$Ni_{0.85}Mo_6Te_8$: INTERATOMIC DISTANCES (STANDARD DEVIATION) IN Å

Mo(1)		Mo(2)		Mo(3)		Ni		Te(1)		Te(2)		Te(3)		Te(4)	
Mo(2)	2.688(1)	Mo(1)	2.688(1)	Mo(1)	2.705(1)	Mo(1)	2.603(3)	Mo(2)	2.779(1)	Mo(1)	2.703(1)	Mo(2)	2.711(1)	Mo(2)	2.721(1)
Mo(3)	2.705(1)	Mo(3)	2.711(1)	Mo(2)	2.711(1)	Mo(3)	2.958(3)	Mo(3)	2.783(1)	Mo(3)	2.758(1)	Mo(3)	2.787(1)	Mo(3)	2.749(1)
Mo(2)	2.748(1)	Mo(1)	2.748(1)	Mo(2)	2.771(1)	Mo(3)	2.985(3)	Mo(1)	2.784(1)	Mo(2)	2.793(1)	Mo(3)	2.827(1)	Mo(1)	2.790(1)
Mo(3)	2.812(1)	Mo(3)	2.771(1)	Mo(1)	2.812(1)	Ni	2.586(6)	Mo(1)	2.850(1)	Mo(2)	2.823(1)	Mo(1)	2.842(1)	Ni	2.426(3)
Mo(1)	3.584(1)	Mo(2)	3.819(1)	Mo(3)	3.631(1)	Te(3)	2.326(3)	Ni	2.442(3)			Ni	2.326(3)		
Mo(1)	3.869(1)	Mo(2)	3.849(1)	Mo(3)	3.934(1)	Te(4)	2.426(3)	Ni	2.655(3)						
Ni	2.603(3)			Ni	2.958(3)	Te(1)	2.442(3)								
				Ni	2.985(3)	Te(1)	2.655(3)								
Te(2)	2.703(1)	Te(3)	2.711(1)	Te(4)	2.749(1)	Te(3)	3.850(3)								
Te(1)	2.784(1)	Te(4)	2.721(1)	Te(2)	2.758(1)										
Te(4)	2.790(1)	Te(1)	2.779(1)	Te(1)	2.783(1)										
Te(3)	2.842(1)	Te(2)	2.793(1)	Te(3)	2.787(1)										
Te(1)	2.850(1)	Te(2)	2.823(1)	Te(3)	2.827(1)										

smaller by 0.03 Å than that in binary Mo_6Se_8 (d_{av}[Mo–Mo] = 2.76 Å (*9*)) (Table II). The Mo_6 clusters interact only weakly with one another ($d_{av,inter}$[Mo–Mo] = 3.68 Å (telluride); 3.31 Å (selenide)). The Ni atoms occupy interstices in the chalcogen atom network and are disordered over pairs of inversion-related sites (occupancy: 0.423(7) and 0.33(−); separation: 2.586(6) Å and 2.279(16) Å for the telluride and selenide,[2] respectively). Their chalcogen atom environments are shown in Fig. 2 and are compared to those of the ternary metal constituents in other triclinic Chevrel phases.

While the Ba atom in $BaMo_6S_8$ (*10*) has eight nearest chalcogen neighbors which form a distorted cube, the Fe atoms in $Fe_2Mo_6S_8$ (*11*) have five which form a distorted square-pyramid, and the Cu atoms in $Cu_{1.8}Mo_6S_8$ (*12*) and the Ni atoms in both $Ni_{0.66}Mo_6Se_8$ (*8*) and $Ni_{0.84}Mo_6Te_8$ each have four which form distorted tetrahedra. Except for Ba all metal atoms are distributed over pairs of inversion-related sites. In the Cu- and Fe-containing compounds these pairs are centered at the cell origin (corresponding to two of the six so-called "inner sites" of the rhombohedral structure (*13*)), and they are far away from the Mo_6 cluster (centered at 1/2, 1/2, 1/2). In the Ni compounds these pairs are centered at the midpoint of one of the cell axes (corresponding to two of the six so-called "outer sites" of the rhombohedral structure), and they are close to the Mo_6 cluster. As shown in Fig. 1 the Ni atoms interact strongly with one Mo_6 cluster via two bonds (d[Ni–Mo] = 2.603(3) Å and 2.958(3) Å (telluride); 2.420(10) Å and 2.824(10) Å (selenide)), and weakly with another via one bond (d[Ni–Mo] = 2.985(3) Å (telluride); 2.862(10) Å (selenide)). Pauling bond order (PBO) sums calculated along the lines described before (*14, 15*) for the various metal–metal bonds in these compounds are summarized in Table III. As expected the contributions of the molybdenum–metal bonds, (Mo-M_x) to the PBO sums are large only for compounds in which the M atoms occupy outer sites, i.e., for those containing Ni, while they are practically zero for compounds in which the M atoms occupy inner sites, i.e., for $Fe_2Mo_6S_8$ (*11*) and $Cu_{1.8}Mo_6S_8$ (*12*), and also for $BaMo_6S_8$ (*10*). The difference between the PBO sums of the Mo–Mo bonds of the Ni-based ternary compounds and those of the corresponding Ni-free binary compounds is larger for the selenide (1.6

[2] Calculated from the lattice constants and atomic parameters reported in Ref. (*8*).

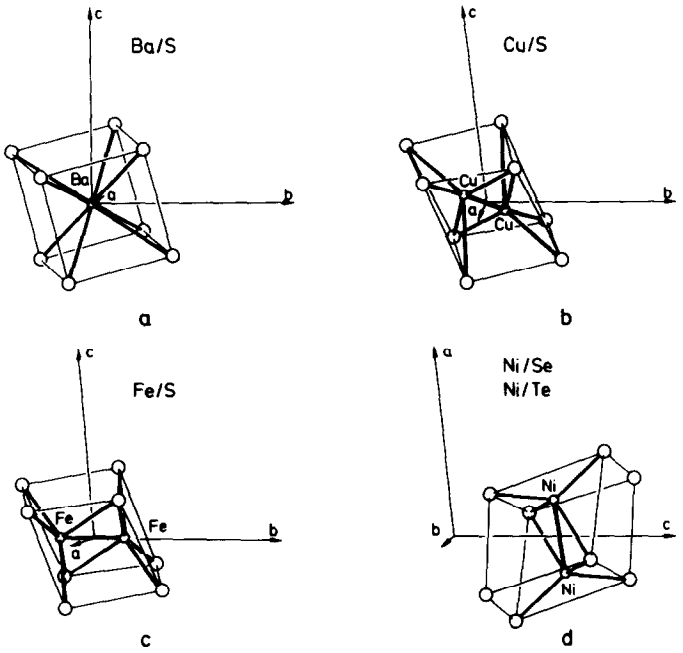

FIG. 2. Comparison between chalcogen atom environments in various triclinic Chevrel phases. (a) $BaMo_6S_8$ (Ba/S), (b) $Cu_{1.8}Mo_6S_8$ (Cu/S), (c) $Fe_2Mo_6S_8$ (Fe/S), (d) $Ni_{0.66}Mo_6Se_8$ (Ni/Se) and $Ni_{0.85}Mo_6Te_8$ (Ni/Te). In each compound the pseudo-trigonal axis runs along [111].

electron pairs) than for the telluride (0.2 electron pair). This is consistent with a previously observed trend concerning the apparent contraction of the Mo_6 clusters due to charge transfer (*13*) and matrix effects (*14*) as one goes from the sulfides to the selenides and tellurides. The relatively large PBO contribution of the metal–metal

TABLE III

PAULING-BOND-ORDER[a] SUMS FOR METAL–METAL BONDS IN TRICLINIC AND RHOMBOHEDRAL CHEVREL PHASES

Compound	Σ(Mo–Mo)[b]	Σ(Mo–M_x)[c]	Σ(M_x–M_x)	Σ + Σ + Σ	Ref.
Mo_6S_8	14.63	—	—	14.63	(*16*)
$BaMo_6S_8$	19.32	0.17	—	19.49	(*10*)
$Fe_2Mo_6S_8$	19.61	0.14	1.16	20.91	(*11*)
$Cu_{1.8}Mo_6S_8$	16.58	0.09	0.14	16.81	(*12*)
Mo_6Se_8	15.11	—	—	13.11	(*9*)
$Ni_{0.66}Mo_6Se_8$	16.69	0.25	2.20	19.14	(*8*)
Mo_6Te_8	15.62	—	—	15.62	(*4*)
$Ni_{0.85}Mo_6Te_8$	15.43	0.12	1.48	17.03	(this work)

[a] Calculated per formula unit by using the relation $d(n) = d(1) - 0.60 \log n$ (n = bond order) and the following atomic radii (Å) for bond order of unity: 1.3095 (Mo), 2.011 (Ba), 1.185 (Fe), 0.955 (Cu), and 1.156 (Ni).

[b] Includes 12 Mo–Mo intracluster and 6 Mo–Mo intercluster bonds.

[c] Includes Mo–M bonds up to 3.5 Å.

bonds, M_x–M_x, in the Fe compound compared to that in the Cu compound is presumably due to the choice of the single-bond radii (Fe: 1.185 Å, Cu: 0.955 Å). Pair formation of the metal atoms has so far only been ascertained for those compounds in which these atoms occupy inner sites, i.e., for $Fe_2Mo_6S_8$ (PP(Fe) = 1.0, d[Fe–Fe] = 2.51 Å (*11*)), and $Cu_{1.8}Mo_6S_8$ (PP(Cu) = 0.90, d[Cu–Cu] = 2.54 Å (*12*)).

Acknowledgments

We thank Drs. K. Peters, W. Bauhofer, and W. J. Westerhaus (all at the Max-Planck Institut für Festkörperforschung, Stuttgart) for data collection, electrical conductivity, and magnetic susceptibility measurements, respectively. This work was partially supported by the Swiss National Science Foundation, Project 2.035-0.86.

References

1. R. CHEVREL AND M. SERGENT, *in* "Superconductivity in Ternary Compounds," Vol. 1, Chapter 2 (Ø. Fischer and M. B. Maple, Eds.), Springer, Berlin 1982.
2. W. HÖNLE AND K. YVON, *Z. Kristallogr.* **162,** 103 (1983).
3. W. HÖNLE, H. G. VON SCHNERING, A. LIPKA, AND K. YVON, *J. Less-Common Met.* **71,** 135 (1980).
4. W. HÖNLE AND H. G. VON SCHNERING, in preparation.
5. G. M. SHELDRICK, SHELXTL, CAMBRIDGE, 1976, unpublished.
6. E. PARTHÉ AND L. GELATO, *Acta Crystallogr. Sect. A* **40,** 169 (1984).
7. "Superconducting Quantum Interference Device," S.H.E. Corp., San Diego (1981).
8. O. BARS, J. GUILLEVIC, AND D. GRANDJEAN, *J. Solid State Chem.* **6,** 335 (1973).
9. O. BARS, J. GUILLEVIC, AND D. GRANDJEAN, *J. Solid State Chem.* **6,** 48 (1973).
10. R. BAILLIF, A. DUNAND, J. MULLER, AND K. YVON, *Phys. Rev. Lett.* **47,** 672 (1981).
11. K. YVON, R. CHEVREL, AND M. SERGENT, *Acta Crystallogr. Sect. B* **36,** 685 (1980).
12. K. YVON, R. BAILLIF, AND R. FLÜKIGER, *Acta Crystallogr. Sect. B* **35,** 2859 (1979).
13. K. YVON, *in* "Current Topics in Materials Science" (E. Kaldis, Ed.), Vol. 3, Chap. 2, North Holland, Amsterdam (1979).
14. J. D. CORBETT, *J. Solid State Chem.* **39,** 56 (1981).
15. W. HÖNLE, H. D. FLACK, AND K. YVON, *J. Solid State Chem.* **49,** 157 (1983).
16. R. CHEVREL, M. SERGENT, AND J. PRIGENT, *Mater. Res. Bull.* **9,** 1487 (1974).